Phytophthora infestans Ago1-associated miRNA promotes potato late blight disease

Xinyi Hu[1]* (ID), Kristian Persson Hodén[1]* (ID), Zhen Liao[1] (ID), Anna Åsman[2]† (ID) and Christina Dixelius[1]† (ID)

[1]Department of Plant Biology, Uppsala BioCenter, Linnean Center for Plant Biology, Swedish University of Agricultural Sciences, PO Box 7080, S-75007 Uppsala, Sweden; [2]Department of Molecular Sciences, Uppsala BioCenter, Linnean Center for Plant Biology, Swedish University of Agricultural Sciences, PO Box 7015, S-75007 Uppsala, Sweden

Summary

• *Phytophthora* spp. cause serious damage to plants by exploiting a large number of effector proteins and small RNAs (sRNAs). Several reports have described modulation of host RNA biogenesis and defence gene expression. Here, we analysed *Phytophthora infestans* Argonaute (Ago) 1 associated small RNAs during potato leaf infection.

• Small RNAs were co-immunoprecipitated, deep sequenced and analysed against the *P. infestans* and potato genomes, followed by transcript analyses and transgenic assays on a predicted target.

• Extensive targeting of potato and pathogen-derived sRNAs to a range of mRNAs was observed, including 638 sequences coding for resistance (R) proteins in the host genome. The single miRNA encoded by *P. infestans* (miR8788) was found to target a potato alpha/beta hydrolase-type encoding gene (*StABH1*), a protein localized to the plasma membrane. Analyses of stable transgenic potato lines harbouring overexpressed *StABH1* or artificial miRNA gene constructs demonstrated the importance of *StABH1* during infection by *P. infestans*. miR8788 knock-down strains showed reduced growth on potato, and elevated *StABH1* expression levels were observed when plants were inoculated with the two knock-down strains compared to the wild-type strain 88069.

• The findings of our study suggest that sRNA encoded by *P. infestans* can affect potato mRNA, thereby expanding our knowledge of the multifaceted strategies this species uses to facilitate infection.

Introduction

Noncoding small RNAs (sRNAs) are known to be important regulators of gene expression. They have been studied extensively in several eukaryotic model species, including Arabidopsis, because they are involved in numerous processes, such as development, maintenance of genome integrity, and stress responses (Axtell, 2013). In plants, 21–24 nucleotide (nt) sRNAs are processed from RNA polymerase II-transcribed primary RNAs (microRNAs or miRNAs) or generated from dsRNA. Among the latter group, secondary small interfering RNAs (siRNAs) such as phasiRNA and tasiRNAs can be formed. The 24-nt siRNAs (p4-siRNAs) which are predominately expressed in developing endosperm are treated as a third main group of sRNAs. At the centre of all these processes are the Dicer-like (DCL), Argonaute (AGO) and RNA dependent RNA polymerase (RDR) protein families. There are, however, distinct differences in sequence formation and preferences, biogenesis and downstream processing of the different sRNA categories. Additional proteins take part in transcriptional and post-transcriptional gene silencing events that

together with the different sRNA classes form a complex picture of the gene regulatory processes, which are excellently reviewed elsewhere (Rogers & Chen, 2013; Matzke & Mosher, 2014; Borges & Martienssen, 2015; Budak & Akpinar, 2015; Fang & Qi, 2016).

Secondary sRNAs constitute a distinct class of sRNAs that are abundant in plants, and they are derived from double-stranded RNA precursors (*PHAS* loci). Their synthesis is triggered by an upstream sRNA-guided transcript cleavage together with successive DCL processing, followed by RDR activity, resulting in phased secondary sRNAs (phasiRNAs). In the Solanaceae plant family, miRNAs can trigger the production of phasiRNAs from resistance (*R*) gene transcripts upon pathogen attack (Li *et al.*, 2012; Shivaprasad *et al.*, 2012). A handful of plant miRNA families are known to govern this response – *R* gene suppression by one such family, miR482/2118, was demonstrated in a comparative study of three tomato species challenged by *Phytophthora infestans* (de Vries *et al.*, 2018). Differentiation among the miRNA family members, including variable activity during the infection process, was observed, as well as variation between the tomato species tested.

In addition to the endogenous regulation of *R* genes, much attention has been given to the mobility of sRNAs within or

between different organisms. Initially, RNA interference in plants was investigated in the context of studies of virus responses. It was shown that virus infection is arrested by the production of DCL-dependent and virus-derived exogenous siRNAs which guide plant AGO proteins to viral RNAs (Guo *et al.*, 2019). To subvert plant defence responses, eukaryotic pathogens can deliver sRNAs during infection, as has been observed in the fungus *Botrytis cinerea* (Weiberg *et al.*, 2013). In this case, the pathogen hijacks the sRNA machinery in *Arabidopsis* with its own sRNAs. However, there are also cases in which, for example, plant miRNAs (miR159 and miR166) can be induced upon fungal infection and cleave fungal effector mRNAs, resulting in resistance, as shown in the interaction between cotton and the vascular fungal pathogen *Verticillium dahliae* in a study by Zhang *et al.* (2016). Although the number of reported cases of plant–pathogen exchange of sRNAs is increasing, there is a lack of deeper understanding of RNA-based interactions between crop species and their major disease-causing agents.

The late blight disease of potato (*Solanum tuberosum*) and tomato (*Solanum lycopersicum*), which is caused by the oomycete *P. infestans*, causes estimated global annual losses of €12 billion (Arora *et al.*, 2014). *Phytophthora infestans* has a large genome enriched in genes coding for effector proteins that promote plant infection by secretion into the apoplastic and cytoplasmic spaces of host tissues (Haas *et al.*, 2019; Whisson *et al.*, 2016). These virulence genes are predominantly located among repeat and transposon sequences, explaining the rapid adaptation potential of this pathogen. Constant changes in *P. infestans* populations and the emergence of new, aggressive strains make disease control, including resistance breeding, extraordinary challenging.

Most of the gene silencing components found in eukaryotic organisms are present in *P. infestans* (*Pi*), such as the proteins encoded by two *DCL* genes (*PiDcl1-2*), five *AGOs* (*PiAgo1-5*) and one gene coding for RDR, *PiRdR1* (Vetukuri *et al.*, 2011; Fahlgren *et al.*, 2013). However, silencing-related proteins such as HUA Enhancer 1 (HEN1), RNA polymerase IV, Drosha and ERI1, which are present in other eukaryotic organisms, are not identified in its genome (Vetukuri *et al.*, 2011). Further, adenine N6-methylation (6mA) has, in both *P. infestans* and *Phytophthora sojae*, replaced the more common 5-methylcytosine DNA-methylation that is implicated in gene regulation (Chen *et al.*, 2018).

The involvement of new functional pathways and/or new candidates within canonical pathways needs to be clarified. The large size of the potato genome (The Potato Genome Sequencing Initiative, 2011; Hardigan *et al.*, 2016) hampers detailed analysis of sRNAs and their predicted targets. In previous studies, 21–24 nt sRNAs have been reported, with 24 nt emerging as the major size class (Lakhotia *et al.*, 2014). The number of components participating in sRNA biogenesis, their functions, and the responses induced upon pathogen attack remain to be established.

Here, we used a *pHAM34:PiAgo1-GFP P. infestans* strain (Åsman *et al.*, 2016) to analyse sRNA-associated events during potato infection. We predicted extensive targeting of potato and pathogen-derived sRNAs to a large number of mRNAs, including 638 sequences coding for R proteins in the host genome.

Intriguingly, the single miRNA in *P. infestans* (miR8788) was found to target an alpha/beta hydrolase-type encoding gene in potato (*StABH1*) whose suppression promotes pathogen growth. *Phytophthora infestans* miR8788 seems to be an ancient molecule, which highlights its conserved role in suppressing the host plant's defence response and further expands the large and diverse repertoire of infection promoting effectors.

Materials and Methods

Materials for Ago-RNA co-immunoprecipitation

Two transformants of *Phytophthora infestans* wildtype (WT) strain 88069 were used (Åsman *et al.*, 2016): one harbouring a green fluorescent protein (GFP)-encoding gene (*pHAM34:GFP*), and the other *P. infestans* Ago1-GFP (*pHAM34:PiAgo1-GFP*). Plant growth conditions, pathogen storage, cultivation and inoculation procedures were as described previously (Vetukuri *et al.*, 2011; Jahan *et al.*, 2015). Three replicates of leaves with lesion sizes between 8 and 12 mm from potato cv Bintje inoculated with either of the two *P. infestans* strains were collected 5 days post inoculation (dpi). For each replicate, 2 g of leaf material was pooled (Supporting Information Fig. S1). Mycelia of the two *P. infestans* strains were grown in pea broth for 7 d, before collecting three mycelia replicates of 200 mg from each strain.

RNA co-immunoprecipitation, sequencing and data analysis

Immunoprecipitation of the collected leaf materials and mycelia was performed (Åsman *et al.*, 2016). Twelve libraries were made at the Ion Proton platform, SciLifeLab (Uppsala, Sweden), where the Ion PI Sequencing 200 Kit v.3 (Life Technologies) was used. Reads were adaptor-trimmed and 18–38 nt reads were mapped to the *P. infestans* genome (Haas *et al.*, 2009) and the *Solanum tuberosum* genome v.4.04 (Hardigan *et al.*, 2016) using Bowtie2 v.2.3.2 (Langmead & Salzberg, 2012). Reads from ribosomal RNA (rRNA), transfer RNA (tRNA) and reads mapping to both the *P. infestans* and the potato genome were discarded. Remaining sRNAs (duplicates excluded) were counted using ShortStack v.3.8.2 (Johnson *et al.*, 2016). The R package DEUS was used for downstream analysis, where an enrichment of at least 2 in $\log_2$ fold change (*P*-value 0.05) compared to the control (*pHAM34:GFP*) was considered significant. No mismatches were allowed and all mapping locations were reported. *Phytophthora infestans* and potato annotations were downloaded from http://protists.ensembl.org/ and http://solanaceae.plantbiology.msu.edu/. Reads mapping to miRNAs were predicted using ShortStack, with the following settings: --strand_cutoff 0.5 --foldsize 1000 --dicermin 18 --dicermax 38. miRNA-like homologs were predicted to major miRNAs by applying the Ssearch algorithm, with a Smith–Waterman score > 90 (Pearson & Lipman, 1988). PhasiRNAs were predicted using PhaseTank v.1.0 (Guo *et al.*, 2015). For pipeline details (see Fig. S2).

sRNA target prediction

To predict sRNA targets in potato, the predicted sRNAs from SHORTSTACK were run in the target analysis server psRNATarget (Dai *et al.*, 2018), against the cDNA library of '*S. tuberosum* transcript, JGI genomic project, Phytozome 12, 448_v4.03' with default settings, except the expectation value was 3. The miR8788 target prediction was run with expectation value 5 (default). sRNA targets in *P. infestans* were predicted using the sRNAs from SHORTSTACK processed in TARGETFINDER (https://github.com/carringtonlab/TargetFinder) against the *P. infestans* genome (Haas *et al.*, 2009), with default settings.

Multiple sequence alignment and phylogeny

The *P. infestans* sRNA target in potato, *StABH1*, and its closest homolog in *Arabidopsis*, *AtABH1*, were further analysed. Sequence homologs with the highest similarity score compared to either StABH1 or AtABH1 (184 + root), were collected from the National Center for Biotechnology Information (NCBI; 15 April 2018) using the BLASTP taxonomy function with default settings. Additional solanaceous sequences were mined from https://solgenomics.net/, http://www.onekp.com, http://www.ebi.ac.uk (PMID: 26442032) and http://www.doi.org/10.5061/dryad.kc835.5. cDNA from the common garden species *Calibrachoa hybrida* was amplified, sequenced (MK550718) and added to the generated sequence dataset. Single-gene maximum likelihood (ML) trees were generated using RAxML v.8.2.11 (Stamatakis, 2006) with the PROTGAMMAJTT and autoMRE settings, including 200 bootstrap replicates. The tree was depicted using the R package GGTREE, and positive selection was tested using PAML v.4.9h (Yang, 2007).

StABH1 cloning, transient expression in *Nicotiana benthamiana*, and Western blotting

Total RNA was isolated from potato using the RNeasy Plant Mini Kit (Qiagen), and cDNA was synthesized with the Maxima cDNA Synthesis Kit (Thermo Fisher Scientific, Waltham, MA, USA) throughout the study. The *StABH1* coding sequence (CDS) was cloned from potato cv Sarpo Mira and fused at the 3′ end to *GFP*, in the binary plasmid pGWB505 (Nakagawa *et al.*, 2007), and transformed into *Agrobacterium* strain GV3101 containing pSoup (Hellens *et al.*, 2000). The *P. infestans* miR8788 stem-loop sequence was amplified from *P. infestans* strain 88069 genomic DNA. The complete stem-loop structure was cloned (Gateway; Invitrogen Life Technologies, Carlsbad, CA, USA) into pGWB505, forming a p35S:GFP-miR8788 construct. All constructs generated in this study were confirmed by Sanger sequencing (Macrogen Inc., Amsterdam, the Netherlands), and all cloning primers are listed in Table S1. Three-week-old *N. benthamiana* plants were used for agroinfiltration. Samples of leaves co-infiltrated with GV3101 (control), empty vector (EV-pGreenII8000, control) and two replicates of miR8788-SL were collected after 3 d and used for Western blot analysis (Åsman *et al.*, 2016), using mouse monoclonal anti-GFP antibody (JL-8; BioNordika, Stockholm, Sweden).

Confocal microscopy

Six-week-old *N. benthamiana* plants were used for all analyses. Plants were agroinfiltrated with pGWB505 containing *p35S*: *StABH1-GFP* and the p19 silencing suppressor (Lindbo, 2007). The same leaves were inoculated with the *P. infestans* strain 88069 tdT (expressing a tandem dimer Tomato fluorescent protein) 1 d post agroinfiltration. Responses were monitored using an LSM780NLO confocal microscope (Zeiss) 3–7 d post agroinfiltration. Excitation/detection wavelengths for GFP and tdT were 488/499–547 nm and 561/589–633 nm, respectively.

Transient transcription dual-luciferase assays

A transient transcription dual-luciferase (Dual-LUC) assay was used (Banerjee *et al.*, 2007; Liu *et al.*, 2008). The ubiquitin-10 promoter was amplified from the plasmid pUBC-GFP Dest (Grefen *et al.*, 2010) and inserted into the *Kpn*I/*Not*I site of pGreenII8000. After *Not*I and *Xba*I digestion, the *StABH1* target sequence (TS) was ligated to the Firefly luciferase CDS. To avoid potential co-suppression, different promoters for REN and LUC were used in the constructs. Primer sequences are provided in Table S1. The *StABH1* mutated target sequence was used as a control. The luciferase activity was analysed using white 96-well plates (Thermo Fisher Scientific), and LUC reaction reagents according to the manufacturer's instruction (Dual-Luciferase Reporter Assay System; Promega). The measurements were performed using an Omega FLUOstar plate reader (BMG Labtech, Ortenberg, Germany) generating quantified LUC values normalized to REN activity (LUC/REN). The experiment was repeated eight times with constant LUC : REN ratios.

5′ RNA ligase-mediated rapid amplification of cDNA ends

5′ RNA ligase-mediated rapid amplification of cDNA ends was performed as follows (McCue *et al.*, 2013): GeneRacer RNA Oligo (Invitrogen) was ligated to the total RNA using T4 RNA ligase (Nordic Biolabs AB, Stockholm, Sweden). cDNA was synthesized and polymerase chain reaction (PCR)-amplified. First, a touchdown PCR with GeneRacer 5′ primer and a gene-specific reverse primer was run. The GeneRacer 5′ nested primer was used for a second PCR, where the first PCR products served as a template. After gel purification, the amplified products were cloned into pJET1.2/blunt (Thermo Fisher Scientific) and sequenced (Macrogen). The oligo sequences are listed in Table S1.

Phytophthora infestans miR8788 knock-down

A miRNA target mimicry approach (Franco-Zorilla *et al.*, 2007; Todesco *et al.*, 2010) was applied to silence the miR8788-3p sequence located in the *PITG_10391* gene. Two target mimics with a modified central sequence were designed (UAGAC nonpairing with UCGCU, MIM8788a; UAGA nonpairing with CGCU, MIM8788b). MIM8788a/MIM8788b show critical mismatches with miR8788 by generating four or five nucleotide

bulges. GFP-MIM8788a/MIM8788b fusions were generated from the pTOR-NGFP vector (Åsman *et al.*, 2016) using Phusion high-fidelity DNA polymerase (Thermo Fisher Scientific) and a reverse GFP cloning primer that contained the miRNA mimicry sequence (MIM8788a or MIM8788b). The PCR product was digested with *Eco*RI and *Not*I, and the fragment was ligated into the corresponding restriction sites in the pTOR-NGFP vector, thereby replacing NGFP. The final insert was 738 bp (717 bp GFP, 21 bp MIM8788a/MIM8788b) and was driven by the *HAM34* promoter. Transformation of the *P. infestans* 88069 WT strain was performed as described previously (Vetukuri *et al.*, 2012), using 50 µg plasmid DNA for each transformation experiment. RNA was extracted from *P. infestans* (88069, *pHAM34:PiAgo1-GFP* and miR8788 knock-down, KD) mycelia using Trizol (Thermo Fisher Scientific). One microgram total RNA was reverse transcribed into cDNA using Maxima Reverse Transcriptase (Thermo Fisher Scientific) as described previously (Chen *et al.*, 2005). The expression of miR8788-5p and -3p was quantified using iTaq Universal SYBR Green Supermix (Bio-Rad) on the CFX Connect Real-Time PCR Detection System (Bio-Rad), using *Pi-Actin A* (PITG_15117) as a reference gene. Relative expression was determined using the 2(Delta-Delta-C(T)) method (Livak & Schmittgen, 2001).

Plant transformation

StABH1 RNAi primers were designed using WMD3 (Web MicroRNA Designer http://wmd3.weigelworld.org/cgi-bin/webapp.cgi). The RNAi vector pRS300 was from Addgene and the *StABH1* amiRNA (*StamiRNA*) precursor was ligated into pGWB505. pGWB505-StABH1 and pGWB505-amiRNA-StABH1 were transformed into potato as outlined previously (Jahan *et al.*, 2015). Both Desirée and Sarpo Mira cultivars were used to ensure production of transformed plants. Ten potential transgenic shoots per construct were grown on Murashige & Skoog (MS) medium containing 20 µg hygromycin B ml^{-1}. Transgenic plants were inoculated with *P. infestans* (strain 88069 on Desirée and for Sarpo Mira strain 11388) as described previously (Jahan *et al.*, 2015). The strain 11388 is very aggressive and has overcome resistance in cv Sarpo Mira, and was thus used for the Sarpo Mira infections. The 88069 strain induces disease in cv Bintje and cv Desirée. RNA was extracted from *P. infestans* inoculated cv Sarpo Mira and cv Desirée leaves, and cDNA was synthesized. Maxima SYBR Green/Fluorescein Master Mix (Thermo Fisher Scientific) was used for the quantitative reverse transcription polymerase chain reaction (qRT-PCR) reactions (iQ5; BioRad) and relative miRNA expression was quantified (Varkonyi-Gasic *et al.*, 2007), using *Pi-Actin A* (PITG_15117) as a reference gene.

Phytophthora infestans DNA quantification

To quantify *P. infestans* DNA in infected leaves, quantitative polymerase chain reaction (qPCR) analysis was carried out essentially as described previously (Llorente *et al.*, 2010). Genomic DNA from infected potato leaves was isolated using cetyltrimethyl ammonium bromide (CTAB) lysis buffer at 65°C for 1 h, followed by phenol/chloroform extraction. For qPCR analysis, 20 ng DNA was used and at least three biological replicates were analysed. *PiO8* was used as a reference gene. Primers are listed in Table S2.

Northern hybridization

Total RNA from potato and *P. infestans* (strains 88069, *pHAM34:PiAgo1-GFP* and *pHAM34:GFP*) was isolated using PureLink Plant RNA Reagent for plant samples (Thermo Fisher Scientific) and Trizol for mycelia samples (Thermo Fisher Scientific). Nineteen µg RNA enriched for the low molecular weight fraction (Kreuze *et al.*, 2005) was resolved on denaturing 12.5% polyacrylamide gels. γ-^{32}P labelled RNA probes (Sigma) (Table S1) were used in Northern hybridization (Åsman *et al.*, 2016). The miR8788 probes and *P. infestans* 5S rRNA probe were hybridized at 42°C, whereas the potato U6 snRNA probe was hybridized at 54°C.

Statistical analysis

Levene's test was used to test for homogeneity of variance across groups (Brown & Forsythe, 1974). When no inequality in variance between samples was found, one of the following three approaches was run in R (https://www.r-project.org), depending on the experimental setup. For pairwise comparisons, Student's unpaired *t*-test was employed. One-way ANOVA was used when analysing the influence of one variable on the difference in means between three or more samples. Experiments examining the influence of two different variables on three or more samples were analysed with two-way ANOVA. Correction for multiple comparisons in any ANOVA test was performed with Tukey's HSD test. Statistical analysis and barplots were generated using the SHINING-QPCR SHINY application (https://github.com/KristianHoden/Shining-qPCR/).

R packages used in this study

The following R packages were used:

AGRICOLAE (v.1.1-3, https://cran.r-project.org/web/packages/agricolae/index.html)

CAR (v.3.0.3, https://cran.r-project.org/web/packages/car/index.html)

CAIRO (v.1.5-12.2, https://cran.r-project.org/web/packages/cairo /index.html)

DEUS (v.1.0, https://timjeske.github.io/DEUS/)

DPLYR (v.1.0.5, https://cran.r-project.org/web/packages/dplyr/index.html)

GGPLOT2 (v.3.3.3, https://cran.r-project.org/web/packages/ggplot2/index.html)

GGSIGNIF (v.0.6.1, https://cran.r-project.org/web/packages/ggsignif/index.html)

GGTREE (v.1.16.6, https://bioconductor.org/packages/release/bioc/html/ggtree.html)

IRANGES (v.2.22.2, https://bioconductor.org/packages/release/bioc/html/IRanges.html)

MULTCOMP (v.1.4-16, https://cran.r-project.org/web/packages/multcomp/index.html)

MULTCOMPVIEW (v.0.1-8, https://cran.r-project.org/web/packages/multcompView/index.html)

ONEWAYTESTS (v.2.4, https://cran.r-project.org/web/packages/onewaytests/index.html)

STATS (v.3.6.1, https://www.R-project.org/)

USERFRIENDLYSCIENCE (v.0.7.2, https://cran.r-project.org/web/packages/userfriendlyscience/index.html)

SHINY (v.1.5.0, https://cran.r-project.org/web/packages/shiny/index.html)

SHINYDASHBOARD (v.0.7.1, https://cran.r-project.org/web/packages/shinydashboard/index.html)

SHINYJQUI (v.0.4.0, https://cran.r-project.org/web/packages/shinyjqui/index.html)

SHINYJS (v.2.0.0, https://cran.r-project.org/web/packages/shinyjs/index.html)

XLSX (v.0.6.5, https://cran.r-project.org/web/packages/xlsx/index.html)

Results

PiAgo1 shifts 5′ nt preference from C to U during infection

We infected potato leaves with the *P. infestans PiAgo1-GFP* strain, and included as controls leaves infected with a strain containing *pHAM34:GFP* (Avrova *et al.*, 2008) (Fig. S1) and mycelia from the two strains grown on plates. Co-immunoprecipitated sRNAs were analysed on an Ion Proton sequencing platform, generating a total of 86 600 701 raw reads. In order to generate detectable *Pi*-sRNA populations, infected leaf materials were collected 5 d post infection. At this time-point, the potato–*P. infestans* interaction has mainly switched into a necrotrophic stage, where potato Argonautes are expressed (Liao *et al.*, 2020).

Computational processing (Fig. S2) resulted in six sRNA datasets comprising 26 123 643 sRNA reads from *P. infestans* and 3 090 568 potato sRNA reads. Analysis of the *P. infestans* sRNA distribution demonstrated size enrichment of 21 nt sRNAs both in the mycelia sample and in the sample from infected potato leaves. The proportion of 21 nt sRNAs was higher in pure mycelia (42 275 reads, 54%) than in the leaf-infected sample (24 088 reads, 39%) (Figs 1a, S3). The overall nt size distribution in the mycelia samples resembled that of previously reported findings (Åsman *et al.*, 2016). The potato sRNA size profile showed enrichment between 18 and 24 nt, with a peak at 21 nt, and a minor presence of sRNAs between 25 and 37 nt (Fig. 1b). Plant miRNAs are known to have a predominant length of 21 nt, particularly from DCL1 processing, while somewhat longer miRNAs are produced by other DCL proteins (Rogers & Chen, 2013). Most plant miRNAs have unique 5′-terminal U nucleotides, a feature selected by AGO1 for the gene silencing process (Mi *et al.*, 2008). A clear U preference was found in PiAgo1-associated sRNAs mapping to potato mRNA (Fig. 1c). The 5′U preference is frequently reported in other organisms, not least in fungi (Thieme *et al.*, 2012; Dahlman & Kück, 2015). The 5′U bias among 21 nt PiAgo1-sRNAs is noteworthy, considering the 5′C preference previously observed among sRNAs of this size class in PiAgo1 at the mycelium stage (Åsman *et al.*, 2016). A 5′C preference was also noted among the total PiAgo1-associated *Pi*-sRNAs during infection (Fig. S4). The frequency of 5′U nt among *Pi*-sRNAs in the infected sample (11%) was more than double that of the mycelia sample. The shift in PiAgo1 5′ nt preference during infection is most likely caused by increased selection for 5′ nt U *Pi*-sRNAs. In detail: the total number of significantly enriched 5′U *Pi*-sRNAs in mycelia (508) is only *c.* 16% of the total number of significantly enriched *Pi*-sRNAs at the infection stage (3217). Among these, only 4% (135) are shared between the datasets. The largest number of 5′U *Pi*-sRNAs from the infection stage are derived from intergenic regions (66%) followed by exons (24%). We hypothesise that this shift in PiAgo1 5′ nt preference during infection could be either an indirect consequence of the 5′U bias of plant 21 nt sRNAs, or a result of a selective preference of PiAgo1 for host miRNAs, the vast majority of which are 21 nt and have 5′U. An intriguing possibility is that PiAgo1 has co-evolved with host miRNA (size and 5′ nt) as a means of efficiently down-regulating selected host genes to favour infection.

mRNAs coding for resistance proteins are the dominant sRNA target

The different *St*-sRNAs loaded into the PiAgo1 pull-down group originated from intergenic regions in the potato genome (64%), exons (27%) and transposable elements (TEs, 5%) (Fig. 1d). Six *St*-miRNAs were encoded in protein-coding genes (four exonic and two intronic) whereas 27 additional *St*-miRNAs originated from intergenic regions. None of the *St*-miRNAs were significantly enriched in the *PiAgo1-GFP* sample compared to the *pHAM34:GFP* control. *St*-miRNA-like RNA were also predicted based on major miRNA similarity. Four *St*-miRNA-like homologs were significantly enriched in the *PiAgo1-GFP* sample compared to the *pHAM34:GFP* control, all originating from potato intergenic regions.

We further predicted mRNA targets and their annotated gene functions in potato for *Pi*-sRNAs, *St*-miRNA-like RNA and a remaining group of *St*-sRNAs. Genes coding for kinases, transferases, resistance proteins and transporters were top-four groups for *Pi*-sRNAs and *St*-sRNAs (Fig. S5). A bias towards the *R* gene category, 616 and 186, was detected in the *Pi*-sRNA and *St*-sRNA datasets. In the *St*-miRNA-like group, four *St*-miRNA-like homologs were predicted to target 21 *St*-genes, where *R* genes, transcription factors, kinases and synthases were the largest groups (Fig. S5). In summary, as many as 638 *R* genes could be potentially down-regulated upon *P. infestans* infection, either by host sRNA biogenesis or by pathogen-derived sRNAs loaded into PiAgo1 (Fig. S6). In the *St*-sRNA and the *Pi*-sRNA datasets, 18 and 45 *R* genes, respectively, were annotated as late blight resistance genes, and five *Rpi-blb2-like* genes were targeted by both sources of sRNAs (Table S3).

The genome of *P. infestans* is rich in TEs (Haas *et al.*, 2009). Long terminal repeat (LTR) retrotransposons were previously found to be a major source of sRNAs in *P. infestans* mycelia
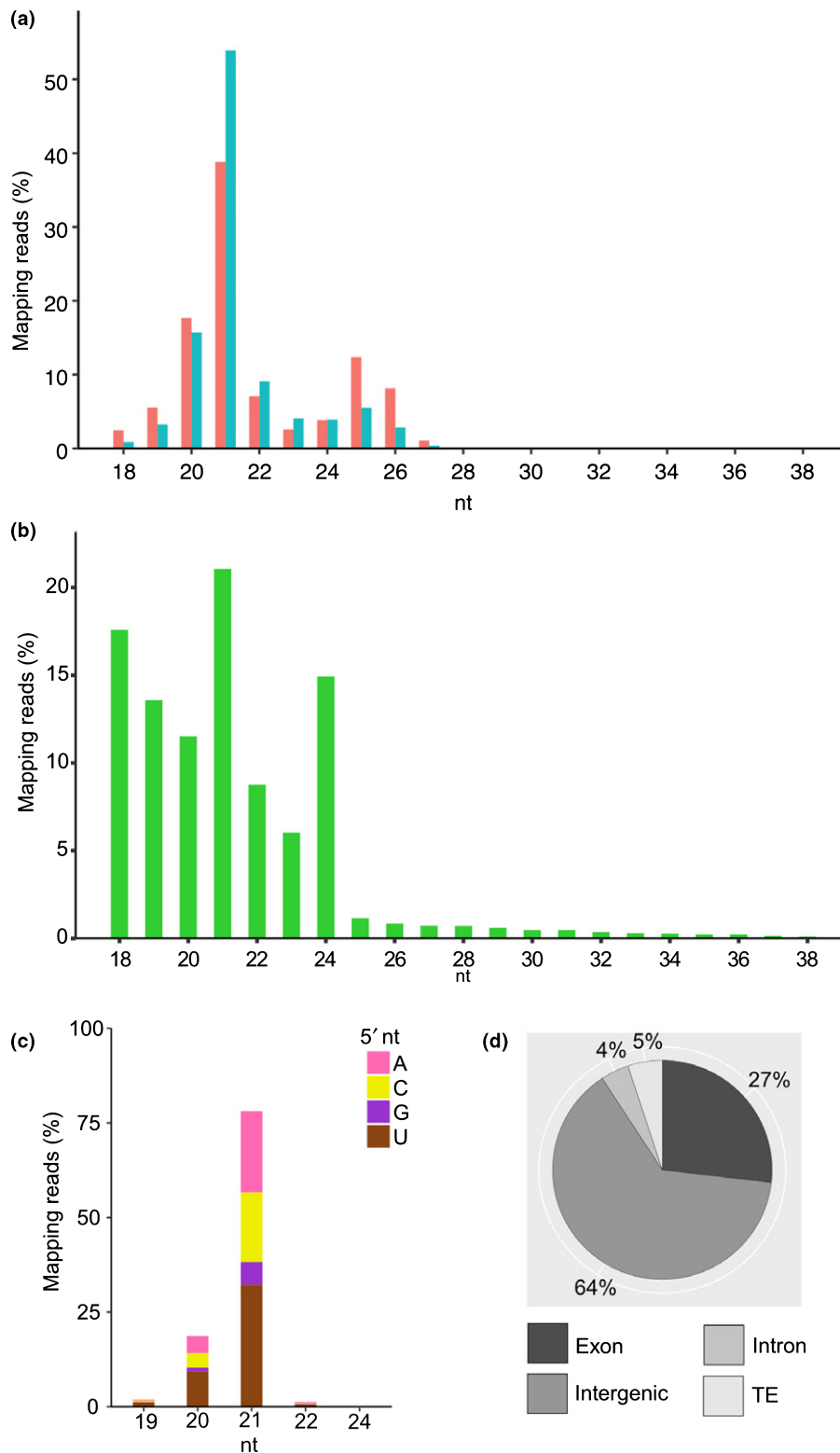
Fig. 1 Characteristics of small RNAs derived from co-immunoprecipitated-enriched RNA samples of *Phytophthora infestans* (*Pi*) Ago1-GFP in mycelia and during infection of potato (*Solanum tuberosum* (*St*)). (a) *Pi*-sRNAs in mycelia (blue, 15 863 929 processed reads) and during potato (cv Bintje) infection (red, 5412 731 processed reads). (b) *St*-sRNAs during potato infection (green, 1432 780 processed reads). (c) Identity of 5′ terminal nucleotide (nt) of *Pi*-sRNAs mapping to potato genes, 5 d post infection. Percentages of *Pi*-sRNAs per nt length, mapping to mRNAs with annotated gene functions, as visualized in Supporting Information Fig. 4(a). Distribution of 5′ U: 61% of 19 nt sRNAs, 50% of 20 nt sRNAs, 41% of 21 nt sRNAs, 35% of 22 nt sRNAs and 100% of 24 nt sRNAs. (d) *St*-sRNAs derived from the potato genome (Hardigan *et al*., 2016). The alignment distribution is as follows: 271 sRNAs to transposable elements (TEs), where retrotransposons dominate (80% of all TEs); 3398 sRNAs to intergenic regions; 1643 sRNAs to genes, comprising 1424 sRNAs to exons and 219 sRNAs to introns. Duplicates were excluded in all datasets.

(Vetukuri *et al.*, 2012). Here, during potato infection and among those *Pi*-sRNAs with potential *R* gene targets, 22% originated from TEs, the majority of which (57%) were from *Gypsy* LTRs. Relative predicted cleavage sites showed a bias towards the 5′ ends of the mRNAs for *R* genes in all three sRNA data sets (Fig. S6).

Among the 7238 sRNAs from *P. infestans*, the only previously confirmed *Pi*-miRNA (miR8788) (Fahlgren *et al.*, 2013) was detected in the *PiAgo1-GFP* infected leaf sample, but not in the *pHAM34:GFP* infected sample. This miRNA is encoded from *PITG_10391*, a gene of unknown function. The miR8788-5p is located in exon 1 and the miR8788-3p in the short (57 nt) intron 1 of *PITG_10391* (Fig. S7). It is worth noting that when searching for information on MIR8788, we found that it was present with an intact pre-miR8788 sequence in raw reads of European herbarium materials collected in 1846 (strain KM177513) and 1877 (strain M-0182896) (Yoshida *et al.*, 2013). MIR8788 is still present in European *P. infestans* strains (Fig. S8), demonstrating its importance for this pathogen. Only pre-miRNA, not *PITG_10391*, is detectable at the genomic level (Fig. S9). Analysis of miR8788 (3p and 5p) revealed that its potential targets are a handful of genes in the *P. infestans* genome (Table S4) and an alpha/beta hydrolase-type encoding gene (PGSC0003DMG 400007679, henceforth *StABH1*) in the potato genome. Only miR8788-3p, and not miR8788-5p, was predicted to target *StABH1,* according to the psRNATarget analysis server.

miR8788 from *P. infestans* induces silencing of *StABH1* mRNA in potato

To validate the predicted miR8788 cleavage site in *StABH1*, 5′ RACE was performed, using total RNA extracted from potato leaves 5 d post inoculation with *P. infestans*. The amplified PCR products, ranging from 100–200 bp, were cloned, sequenced and mapped to the potato genome (Hardigan *et al.*, 2016). One out of 10 clones terminated at the predicted cleavage site in *StABH1* (Fig. 2a,b), suggesting miRNA-induced silencing through a cleavage-independent mechanism, such as translational repression (Yang *et al.*, 2021). 5′ RACE on total RNA extracted from potato inoculated with water resulted in 40 clones, none of which indicated *StABH1* cleavage without *P. infestans* (Figs 2c, S7). This result was followed up by Northern hybridization, demonstrating the presence of miR8788-5p in *PiAgo1-GFP* infected potato (Fig. 2d). Involvement of any phasiRNA generated from potato *R* genes was also checked. Eighty-five phasiRNA loci were identified (Fig. S10) and sRNA from two of these were significantly enriched. However, no candidate was detected that might interfere with *StABH1*. Next, the dual-luciferase reporter system was used with agroinfiltrated *N. benthamiana* leaf materials (Fig. 3a). This approach generated repression of the target mRNA sequence (Fig. 3b) also seen in Western blot analysis (Fig. 3c). Alternative miR8788 targets were searched for and three potential sequence candidates were analysed, but no cleavages were detected at the predicted miRNA sites by 5′ RACE (Fig. S7). Throughout our work, *Pi*-miR8788-3p has for some inexplicable reason not been possible to detect

by Northern blot, although it is present in the *pHAM34:PiAgo1-GFP* co-IP datasets. Equal levels of miR8788-5p and miR8788-3p were observed in agroinfiltrated *N. benthamiana* leaves (Fig. 3d), highlighting the importance of analysis in a correct biological context (e.g. in a suitable host and in presence of the pathogen) to differentiate the active from the inactive miRNA species. The two fragments seen in the Northern blot (Fig. 2d) correspond to 19 nt and 21 nt 3′ isomiRs of miR8788-5p, and are also present in our PiAgo1 co-IP datasets (Fig. S11).

StABH1 is localised to the plasma membrane

The miR8788 target in potato *StABH1* was further analysed. The *St*ABH1 protein has a single trans-membrane domain and an alpha/beta hydrolase fold domain and is significantly suppressed in potato upon *P. infestans* inoculation (Fig. S12). To monitor *St*ABH1 localization in *N. benthamiana* cells, a GFP-tag was fused to the C-terminus of *St*ABH1 followed by agroinfiltration. A *P. infestans* strain expressing tandem dimer Tomato (tdT) fluorescent protein was inoculated on the same leaves, 1 d post agroinfiltration. StABH1-GFP was observed at the plasma membrane of uninfected *N. benthamiana* cells (Fig. S13a). After 4 d, the signal from transmembrane bound *St*ABH1-GFP started to decrease, whereas the number of cytosolic bodies labelled by StABH1-GFP increased in the *P. infestans-tdT* infected tissue. The translocation process continued until at least day seven (Fig. S13b). This picture corresponds to previous reports of intracellular events for a subset of RXLR effectors (S. Wang *et al.*, 2019).

*St*ABH1 is member of a small family of two genes (Figs S14, S15) located in different *Solanaceae* clades of the ABH superfamily, which is known for its diverse functions (Mindrebo *et al.*, 2016). No positive selection could be detected for any amino acid of *St*ABH1 nor for the *St*ABH1 branch using site models implemented in PAML (Yang, 2007). *StABH1* is present in seven common potato cultivars, and the miR8788 target site was found in all genotypes (Fig. S16). In summary, we propose that *St*ABH1 is a conserved multifunctional protein with critical cellular functions in potato and other plant species.

StABH1 is a critical defence component against *P. infestans*

Stable transgenic potato lines were produced using *Agrobacterium*-mediated transformation, first using the same *StABH1* over-expression (OE) construct as in the transient *N. benthamiana* assay (Fig. 4a,b). These plants were used to determine the disease response to *P. infestans*. Inoculated leaves showed significantly smaller disease lesions and less growth of *P. infestans*, after 5 d compared to WT (Fig. 4b,c). At the same time-point, the *StABH1* transcript level was about 10-fold lower compared to mock treatment in the OE lines (Fig. 4d). Although we cannot exclude the involvement of an endogenous host factor in *StABH1* silencing, the data indicate that StABH1 plays a critical role in defence against *P. infestans*. We also generated stable potato transgenic lines containing an artificial miRNA (*StamiRNA*) construct to induce silencing of the *StABH1*
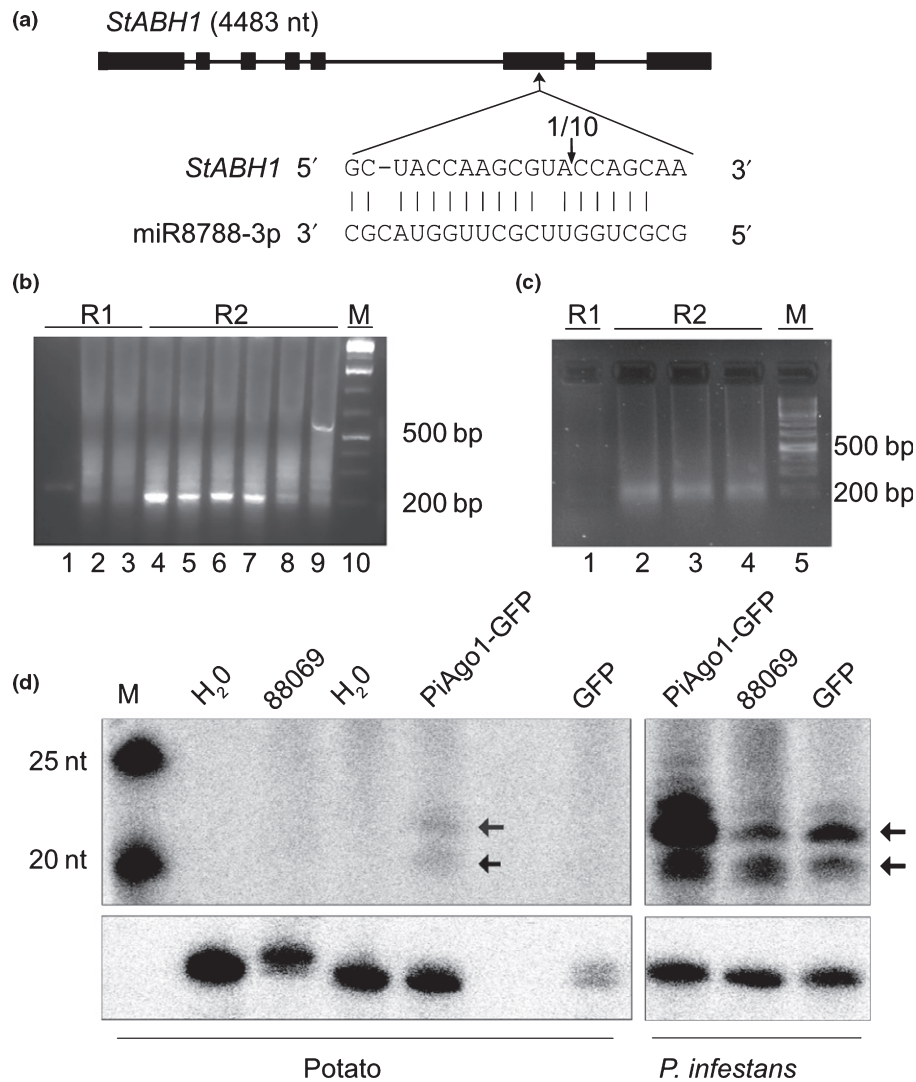
Fig. 2 *StABH1* down-regulation is controlled by miR8788. (a) Schematic drawing showing the exons (filled boxes) and introns (black lines) in the *StABH1* alpha/beta hydrolase-type encoding gene in potato, and the alignment of miR8788-3p with *StABH1* at the predicted binding site. The arrow with the fraction '1/10' above it indicates the number of identical clones detected by 5′ rapid amplification of cDNA ends (5′ RACE) at the computer-predicted cleavage site. (b) The 5′ RACE products of *StABH1* in *Phytophthora infestans*-infected potato (cv Bintje). R1 (lane 1–3) produced using GeneRacer 5′ primer and target mRNA 3′ primer; R2 (lane 4–9), miR8788-specific product generated with GeneRacer 5′ nested primer and target mRNA 3′ primer. (c) The 5′ RACE products of *StABH1* in water-inoculated potato (cv Bintje). R1 (lane 1) produced using GeneRacer 5′ primer and target mRNA 3′ primer; R2 (lane 2–4), products generated with GeneRacer 5′ nested primer and target mRNA 3′ primer. M = 1 kb plus DNA. (d) Northern blot analysis using a γ-^{32}P labelled RNA probe for miR8788-5p. M = γ-^{32}P-labelled GeneRuler Ultra Low Range DNA Ladder. H_2O = water inoculation. *Phytophthora infestans* infected potato leaves (with strains 88069, pHAM34:PiAgo1-GFP and pHAM34:GFP). Infected materials were collected 5 d post inoculation (dpi). IsomiRs of miR8788-5p (19 and 21 nt) are indicated with black arrows. The lower panel depicts U6 snRNA from potato (loading control, probe cross-reacts with *P. infestans* U6).

transcript (Fig. 4e,f). In contrast to our OE materials, *P. infestans* spread quickly in these transgenic lines (Fig. 4f). As soon as 2 d after inoculation, sporangiophores started to protrude from the leaves. After 3 d, many leaves were completely covered with mycelia, sporangiophores and sporangia. The DNA content of *P. infestans* was also significantly higher in the *StamiRNA* plants when *StABH1* was knocked-down compared to *StABH1* in wild-type potatoes (Fig. 4g). Similarly, the *StABH1* transcript level was significantly reduced in the *StamiRNA* plants (Fig. 4h). A miRNA target mimic approach was next applied to inhibit miR8788 activity in *P. infestans*. Six KD candidates were identified, and KD1 and KD5 showed reduced miR8788 levels

(Fig. 5a,b). Next, the impact on *StABH1* in potato leaves was monitored, and elevated *StABH1* expression levels were observed when leaves were inoculated with the two KD strains compared to the WT strain (Fig. 5c,d). The disease lesion size was significantly reduced in leaves infected by the KD strains (Fig. 5e,f). In summary, the plant–pathogen responses observed are consistent with reduced exposure to miR8788 activity.

Discussion

sRNAs have emerged as important endogenous gene regulators in both microbes and plants, not least in various stress

Fig. 3 *StABH1* silencing by miR8788 is confirmed by Luciferase reporter assay. (a) T-DNA constructs used in the luciferase reporter assay. 35S, 35S promoter; LUC, firefly luciferase; NosT, Nos 3′ terminator; NS, non-specific sequence; REN, Renilla luciferase; TS, miR8788 target sequence in *StABH1*; Ubi-10, Ubi-10 promoter. (b) Luciferase reporter assay in *Nicotiana benthamiana* samples, 3 d post agroinfiltration. Dark grey bars represent agroinfiltration with GV3101; light grey bars represent agroinfiltration with the silencing construct (SC). Reporters: *p35S:REN:LUC*(TS), *p35S:REN:LUC* (NS). The quantified LUC normalized to REN activities are shown (LUC/REN). Error bars indicate mean ± SE of the mean (*n* = 10, df = 18). Asterisks indicate significant difference between the reporters during agroinfiltration with the SC (Student's *t*-test; ***, *P* < 0.001). (c) Detection of StABH1-GFP protein co-infiltrated with GV3101 (control), empty vector (EV; pGreenII8000, control) and two replicates of miR8788-SL. Negative, no infiltration (control); NS, non-specific (*Nicotiana benthamiana* Rubisco protein). Samples in the Western blot were probed with anti-GFP antibody. (d) Relative transcript levels of miR8788-5p (yellow) and miR8788-3p (purple) in *N. benthamiana*, 3 d post miR8788-SL agroinfiltration. Error bars indicate mean ± SE of the mean (*n* = 4, df = 6). Student's *t*-test shows no significant difference. *NtActin* was used as a reference gene.

situations. *Phytophthora infestans* has a genome organization in which core genes of biological importance are located in transposon-poor regions, whereas effector-encoding genes are located in transposon-rich regions, which are prone to rapid diversification (Haas *et al.*, 2009). This genomic setting promotes rapid adaptation to resistance breeding and in some countries also to agrochemical treatments (Leesutthiphonchai *et al.*, 2018). In addition to the numerous RXLR and CRN effectors that are predicted in the genome, additional molecules, such as cell wall degrading enzymes, are known to assist in the infection process. It is still unclear how the effectors are regulated. One suggestion is based on the idea that sRNAs that are homologous to transposable elements may lead to the suppression of nearby genes (Vetukuri *et al.*, 2012; Whisson *et al.*, 2012; Fahlgren *et al.*, 2013). sRNAs are also known to be associated with RXLR gene silencing (Vetukuri *et al.*, 2012; Fahlgren *et al.*, 2013; Qutob *et al.*, 2013; Jia *et al.*, 2017) and were recently shown to regulate the RXLR effector *Avr1b* in *P. sojae* (Q. Wang *et al.*, 2019). Genome analysis of *P. sojae* further suggested that sRNAs generated by bidirectional transcription of *Avr1b* are responsible for changes in virulence among isolates.

The intimate contact between pathogen and plant cells favours communications such as cross-kingdom trafficking of sRNA molecules. Knowledge of sRNA translocation events is emerging from several plant–microbe systems (Hudzik *et al.*, 2020), including Rhizobium, which delivers tRNA-derived sRNA fragments (tRFs) into soybeans to promote nodulation (Ren *et al.*, 2019). This process is channelled through AGO1-hijacking, leading to host gene suppression among oomycetes exemplified by *Hyaloperonospora arabidopsidis* (Dunker *et al.*, 2020). Similar examples have been documented for viruses, bacteria and fungi, where effectors have evolved that inhibit plant RNA silencing pathways (reviewed by Pumplin & Voinnet, 2013; Huang, *et al.*, 2019).

In oomycetes, the RXLR effector named '*Phytophthora sojae* (*Ps*) suppressor of RNA silencing 2' (PsPSR2) promotes infection in soybean (Qiao *et al.*, 2013). A similar function has been reported for a homolog of *P. infestans* (PiPSR2) (Xiong *et al.*, 2014). Analysis of the protein structure of PsPR2 revealed seven tandem repeat units, including one W-Y motif and six L-W-Y motifs, features common to 293 effectors among five *Phytophthora* species but with variable numbers of L-W-Y units (He *et al.*, 2019). The L-W-Y units are suggested to be of importance for virulence function and to contribute to the effector diversity
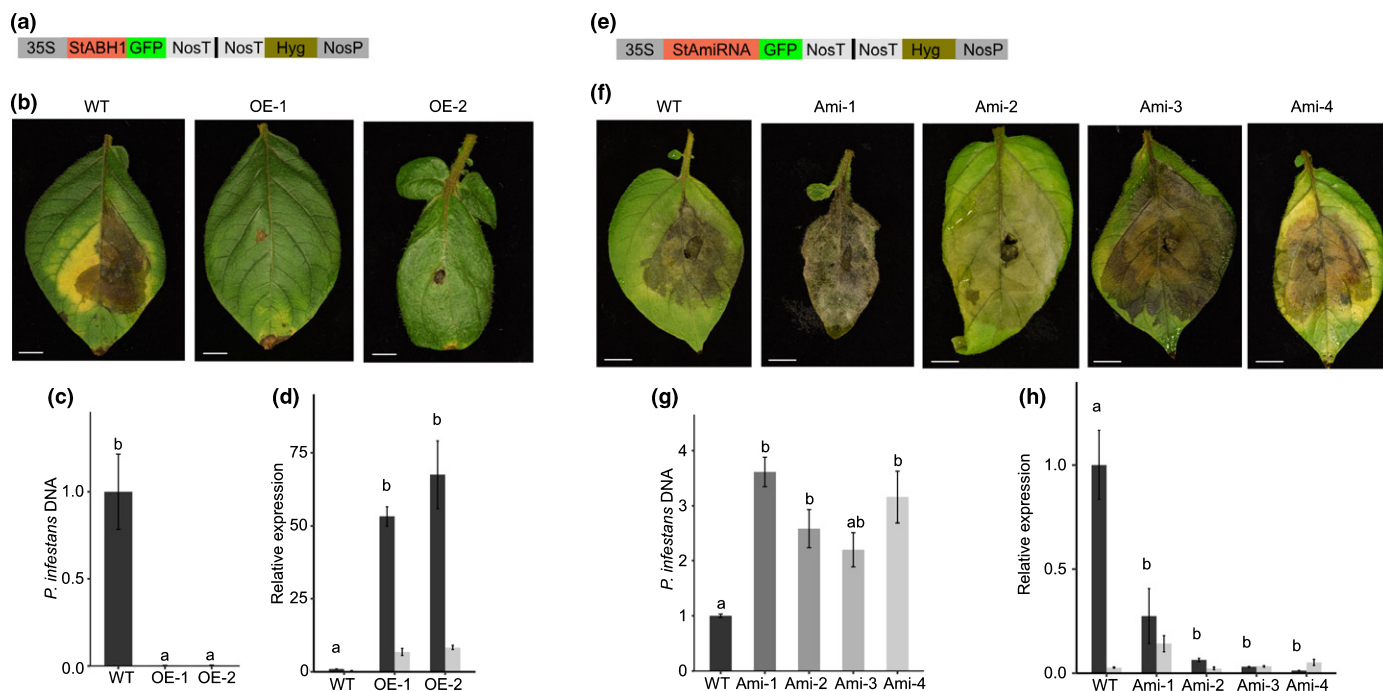
Fig. 4 *StABH1* is essential for potato defence against *Phytophthora infestans*. (a) Construct used to produce *StABH1* over-expression lines: 35S, 35S promoter; GFP, green fluorescent protein; Hyg, hygromycin B resistance gene; NosP, nos promoter; NosT, nos 3′ terminator. (b) Disease phenotype of wild-type (WT; cv Sarpo Mira, strain 11388) and two transgenic over-expression lines containing the *p35S:StABH-GFP* construct (OE-1, OE-2), inoculated with *P. infestans*. Bars, 1 cm. (c) Relative *P. infestans* DNA content in leaves from the over-expression potato lines in (b). Error bars indicate mean ± standard error of the mean ($n = 3$, $df = 8$). Lowercase letters (a, b) in the bar chart represent significant differences (one-way ANOVA and Tukey's HSD test; $P < 0.001$). *PiO8* was used as a reference gene. (d) Relative expression of *StABH1* in leaves from the over-expression lines in (b), when inoculated with water (black) or *P. infestans* (grey). Error bars indicate mean ± SE of the mean ($n = 3$, $df = 17$). Lowercase letters (a, b) in the bar chart represent significant differences (two-way ANOVA and Tukey's HSD test; $P < 0.001$). *StActin* was used as a reference gene. (e) Construct used to produce transgenic artificial miRNA lines: 35S, 35S promoter; GFP, green fluorescent protein; Hyg, hygromycin B resistance gene; NosP, nos promoter; NosT, nos 3′ terminator; StamiRNA, potato artificial miRNA (f) Disease phenotype of wild-type (WT; cv Desirée, strain 88069) and four transgenic artificial miRNA potato lines (Ami-1, Ami-2, Ami-3, Ami-4) inoculated with *P. infestans*. Bars, 1 cm. (g) Relative *P. infestans* DNA content in leaves from the artificial miRNA lines in (f). Error bars indicate mean ± SE of the mean ($n = 3$, $df = 14$). Lowercase letters (a, b) in the bar chart represent significant differences (one-way ANOVA and Tukey's HSD test: $P < 0.05$). *PiO8* was used as a reference gene. (h) Relative expression of *StABH1* in leaves from the artificial miRNA potato lines in (f), during inoculation with water (black) or *P. infestans* (grey). Error bars indicate mean ± SE of the mean ($n = 3$, $df = 19$). Lowercase letters (a, b) in the bar chart represent significant differences (two-way ANOVA and Tukey's HSD test; $P < 0.001$). *StActin* was used as a reference gene.

observed in genome-wide analyses of diverse oomycetes. A suppressor of RNA silencing 1 (PSR1) is known to bind to a nuclear host protein (PINP1) encoding a DEAH-box RNA helicase domain that regulates the accumulation of miRNAs and endogenous Arabidopsis sRNAs (Qiao *et al.*, 2015). Silencing of *PINP1* in *N. benthamiana* resulted in decreased plant sRNA levels and hyper-susceptibility to *P. infestans*. In our datasets, sequence homologs of *PiPSR2*, *PSR1* and its interacting protein 1 (*PINP1*) were searched for. Out of the five most homologous sequences to *PSR1*, only PITG_16275 was found to be upregulated upon potato infection. However, enrichment of *Pi*-sRNAs ($\log_2 FC > 2$, $P < 0.05$, compared to the *pHAM34:GFP* control) from *P. infestans* that are predicted to target PITG_16275 during infection suggests complex, multi-layered regulation. No differential expression when comparing mycelia and infected samples was observed for the corresponding candidate to *PSR2* (PITG_15152).

The potato–*P. infestans* interaction seems to differ somewhat from the Arabidopsis–*Phytophthora capsici* system, where secondary siRNAs from pentatricopeptide-repeat protein (*PPR*)-encoding gene loci in Arabidopsis are translocated in extracellular vesicles to *P. capsici* and target pathogenicity genes upon infection (Hou *et al.*, 2019). As a counter response, PsPSR2 blocks this action via the suppression of secondary siRNA biogenesis in the plant. In potato, *PPR* sRNAs are predicted to target an *RXLR* (*PITG_14884*) and a gene coding for a signal peptide domain protein with RXLR effector similarity (*PITG_06080*). However, no difference in expression levels was seen in *PiPSR2* during infection in our datasets.

In plants, sRNAs are known to move intercellularly and systemically, and are transported through plasmodesmata and phloem (Liu & Chen, 2018). A plant protein known to mediate cell-to-cell movement of sRNA is phloem small RNA binding protein 1 (CmPSRP1), which was initially identified in pumpkin (Yoo *et al.*, 2004). Long-distance trafficking is mediated via the formation of a ribonucleoprotein complex whose stability is regulated by CmPSRP1 phosphorylation (Ham *et al.*, 2014). Glycin-rich domains in PSRP1 homologs of Arabidopsis have been shown to be required for the 'movement' function
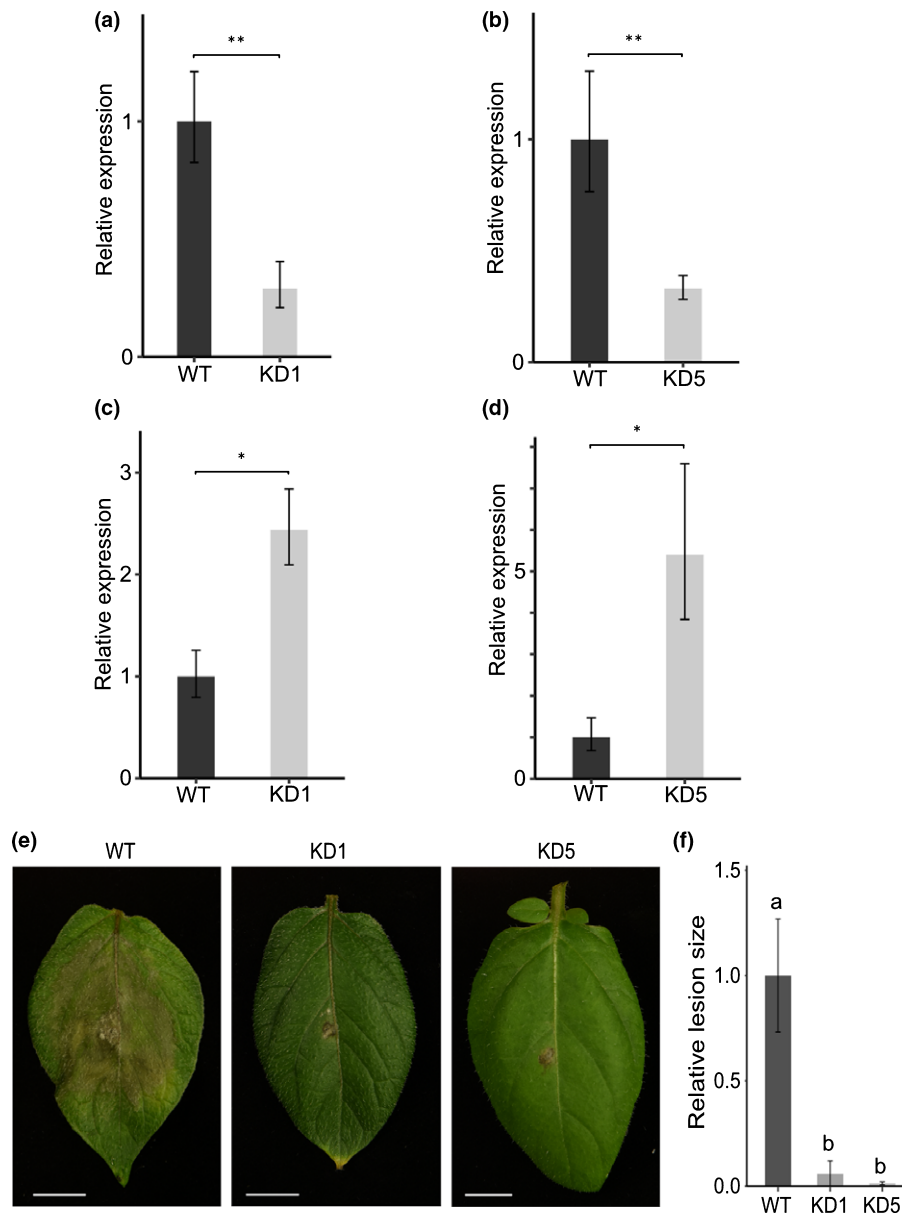
Fig. 5 *Phytophthora infestans* miR8788-3p knock-down strains show impaired *StABH1* silencing. (a) Relative transcript levels of miR8788-3p in 88069 (WT) and miR8788 knock-down (KD1) mycelia. Error bars indicate mean $\pm$ SE of the mean ($n = 8$, df = 14). (b) Relative transcript levels of miR8788-3p in 88069 (WT) and miR8788 knock-down (KD5) mycelia. Error bars indicate mean $\pm$ SE of the mean ($n = 4$, df = 6). (c) Relative transcript levels of *StABH1* in leaves during infection by the *P. infestans* strains 88069 (WT) and KD1; error bars indicate mean $\pm$ SE of the mean ($n = 4$, df = 6). (d) Relative transcript levels of *StABH1* in leaves during infection by *P. infestans* strains 88069 (WT) and KD5. Error bars indicate mean $\pm$ SE of the mean ($n = 7$, df = 12). *PiActin* and *StActin* were used as reference genes. Asterisks indicate significant differences between transcript levels according to Student's *t*-test (*, $P < 0.05$; **, $P < 0.01$). (e) Disease phenotype of *P. infestans* strains 88069 (WT), KD1 and KD5. Bars, 1 cm. (f) Relative lesion size on leaves inoculated with *P. infestans* strains 88069 (WT), KD1 and KD5. Error bars indicate mean $\pm$ SE of the mean ($n = 22$, df = 65). Lowercase letters in the bar chart (a, b) represent significant differences (one-way ANOVA and Tukey's HSD test; $P < 0.001$). All disease data (c–f) are from potato leaves of cv Desireé, 5 d post inoculation.

(Yan *et al.*, 2020). When searching for the closest related sequence to *CmPSRP1* in the potato genome, we found PGSC0003DMP400030419, a gene with low sequence identity (23.6%) to *CmPSRP1*. This suggests that another/other gene candidate(s) may be involved in such transport events in potato if a similar mechanism is present.

Small membrane vesicles such as exosomes of endocytic origin deliver a wide range of cargo from the cell to the intercellular

space (Théry, 2011). These transport entities or extracellular vesicles (EVs) are thought to be conserved among all organisms and function to keep cellular homeostasis. However, they also hold key roles in cellular communication (Rybak & Robatzek, 2019), and recent studies have pointed to important roles in plant–pathogen interactions. Extracellular vesicle mediated sRNA trafficking from Arabidopsis to *B. cinerea* has been demonstrated (Cai *et al.*, 2018), as well as from Arabidopsis to *P. capsici*

New
Phytologist

(Hou *et al.*, 2019). Whether the reverse transport from pathogen to plant also occurs via EVs is currently unclear. *P. infestans* expresses > 400 transporters, but none is specifically located to haustoria (Ah-Fong *et al.*, 2017) and it is believed that nutrients from the host are acquired from the apoplast.

A recent study suggests that *P. infestans* enhances endosomal trafficking during infection and that the PexRD12/31 effectors co-localize with the vesicle machinery (Petre *et al.*, 2021).

If and how StABH1 impacts on such processes is presently not understood. Likewise, it is not clear how sRNAs are translocated between *P. infestans* and potato. The possibility that such molecules could be secreted via specific transporters and then incorporated in the host vesicle system cannot be excluded.

It can be concluded that hundreds of potato genes, particularly *R* genes, are predicted sRNA targets during *P. infestans* infection, and this response has been documented here, as well as in previous work (de Vries *et al.*, 2018). Cascades of different sRNA classes, including secondary sRNAs from *R* genes, are also observed in tomato plants infected with *P. infestans* (Canto-Pastor *et al.*, 2019). As a note of concern, the numbers of plant sRNA targets predicted from sRNA-seq studies might be large overestimates. When we reprocessed data from this study together with additional sequence information, the number of targeted *R* genes dropped to only seven (Persson Hodén *et al.*, 2021). This study has revealed a novel tool in the *P. infestans* infection toolbox – miR8788-induced suppression of the potato defence-associated gene *ABH1*. Many sRNA-related processes remain to be elucidated, including *trans*-organism transport, molecular targeting mechanisms and the extent of transcriptional reprogramming.

Acknowledgements

Author contributions

XH, AÅ, KPH, and ZL performed experiments and analysed data; XH, AÅ, KPH, ZL and CD designed experiments; CD, KPH and AÅ wrote the manuscript. XH & KPH and AÅ & CD contributed equally to this work.

ORCID

Anna Åsman https://orcid.org/0000-0002-7905-6853
Christina Dixelius https://orcid.org/0000-0003-0150-0608
Xinyi Hu https://orcid.org/0000-0003-2259-8667
Zhen Liao https://orcid.org/0000-0002-0282-7787
Kristian Persson Hodén https://orcid.org/0000-0003-0354-0662

Data availability

References

Ah-Fong AMV, Shrivastava J, Judelson HS. 2017. Lifestyle, gene gain and loss, and transcriptional remodeling cause divergence in the transcriptomes of *Phytophthora infestans* and *Pythium ultimum* during potato tuber colonization. *BMC Genomics* **18**: 764.

Arora R, Sharma S, Singh BP. 2014. Late blight disease of potato and its management. *Potato Journal* **41**: 16–40.

Åsman AKM, Fogelqvist J, Vetukuri R, Dixelius C. 2016. *Phytophthora infestans* Argonaute 1 binds microRNA and small RNAs from effector genes and transposable elements. *New Phytologist* **211**: 993–1007.

Avrova AO, Boevink PC, Young V, Grenville-Briggs LJ, van West P, Birch PRJ, Whisson SC. 2008. A novel *Phytophthora infestans* haustorium-specific membrane protein is required for infection of potato. *Cellular Microbiology* **10**: 2271–2284.

Axtell MJ. 2013. Classification and comparison of small RNAs from plants. *Annual Review of Plant Biology* **64**: 137–159.

Banerjee R, Schleicher E, Meier S, Viana RM, Pokorny R, Ahmad M, Bittl R, Batschauer A. 2007. The signaling state of Arabidopsis cryptochrome 2 contains flavin semiquinone. *Journal of Biological Chemistry* **282**: 14916–14922.

Borges F, Martienssen RA. 2015. The expanding world of small RNAs in plants. *Nature Review of Molecular Cell Biology* **16**: 727–741.

Brown MB, Forsythe AB. 1974. Robust tests for the equality of variances. *Journal of American Statistical Association* **69**: 364–367.

Budak H, Akpinar BA. 2015. Plant miRNAs: biogenesis, organization and origins. *Functional Integrative Genomics* **15**: 523–531.

Cai Q, Qiao L, Wang M, He B, Lin FM, Palmquist J, Huang SD, Jin H. 2018. Plants send small RNAs in extracellular vesicles to fungal pathogen to silence virulence genes. *Science* **360**: 1126–1129.

Canto-Pastor A, Santos BAM, Walli AA, Summers W, Schornack S, Baulcome DC. 2019. Enhanced resistance to bacterial and oomycete pathogens by short tandem target mimic RNAs in tomato. *Proceedings of the National Academy of Sciences, USA* **116**: 2755–2760.

Chen C, Ridzon DA, Broomer AJ, Zhou Z, Lee DH, Nguyen JT, Barbisin M, Xu NL, Makuvakar VR, Andersen MR *et al.* 2005. Real-time quantification of microRNAs by stem-loop RT-PCR. *Nucleic Acids Research* **33**: e179.

Chen H, Shu H, Wang L, Zhang F, Li XI, Ochola SO, Mao F, Ma H, Ye W, Gu T *et al.* 2018. *Phytophthora* methylomes are modulated by 6mA methyltransferases and associated with adaptive genome regions. *BMC Genome Biology* **19**: 181.

Dahlmann TA, Kück U. 2015. Dicer-dependent biogenesis of small RNAs and evidence for microRNA-like RNAs in the penicillin producing fungus *Penicillium chrysogenum*. *PLoS ONE* **10**: e0125989.

Dai X, Zhuang Z, Zhao PX. 2018. psRNATarget: a plant small RNA target analysis server (2017 release). *Nucleic Acids Research* **46**: W49–W54.

Dunker F, Trutzenberg A, Rothenpieler JS, Kuhn S, Pröls R, Schreiber T, Tissier A, Kemen A, Kemen E, Hückelhoven R *et al.* 2020. Oomycete small RNAs bind to the plant RNA-induced silencing complex for virulence. *eLife* 9: e56096.

Fahlgren N, Bollmann SR, Kasschau KD, Cuperus JT, Press CM, Sullivan CM, Chapman EJ, Hoyer JS, Gilbert KB, Grünwald NJ *et al.* 2013. *Phytophthora* have distinct endogenous small RNA populations that include short interfering and microRNAs. *PLoS ONE* 8: e77181.

Fang X, Qi Y. 2016. RNAi in plants: an Argonaute-centered view. *Plant Cell* 28: 272–285.

Franco-Zorrilla JM, Valli A, Todesco M, Mateos I, Puga MI, Rubio-Somoza I, Leyva A, Weigel D, Garcia JA, Paz-Ares J. 2007. Target mimicry provides a new mechanism for regulation of microRNA activity. *Nature Genetics* 39: 1033–1037.

Grefen C, Donald N, Hashimoto K, Kudla J, Schumacher K, Blatt MR. 2010. A ubiquitin-10 promoter-based vector set for fluorescent protein tagging facilitates temporal stability and native protein distribution in transient and stable expression studies. *The Plant Journal* 64: 355–365.

Guo Q, Qu X, Jin W. 2015. PHASETANK: genome-wide computational identification of phasiRNAs and their regulatory cascades. *Bioinformatics* 31: 284–286.

Guo Z, Li Y, Ding S-W. 2019. Small RNA-based antimicrobial immunity. *Nature Review of Immunology* 19: 31–44.

Haas BJ, Kamoun S, Zody MC, Jiang RH, Handsaker RE, Cano LM, Grabherr M, Kodira CD, Raffaele S, Torto-Alalibo T *et al.* 2009. Genome sequence and analysis of the Irish potato famine pathogen *Phytophthora infestans*. *Nature* 461: 393–398.

Ham BK, Li G, Jia W, Leary JA, Lucas WJ 2014. Systemic delivery of siRNA in pumpkin by a plant PHLOEM SMALL RNA-BINDING PROTEIN 1-ribonucleoprotein complex. *The Plant Journal* 80: 683–694.

Hardigan MA, Crisovan E, Hamilton JP, Kim J, Laimbeer P, Leisner CP, Manrique-Carpintero NC, Newton L, Pham GM, Vaillancourt B *et al.* 2016. Genome reduction uncovers a large dispensable genome and adaptive role for copy number variation in asexually propagated *Solanum tuberosum*. *Plant Cell* 28: 388–405.

He J, Ye W, Choi DS, Wu B, Zhai Y, Guo B, Duan S, Wang Y, Gan J, Ma W, Ma J. 2019. Structural analysis of *Phytophthora* suppressor of RNA silencing 2 (PSR2) reveals a conserved modular fold contributing to virulence. *Proceedings of the National Academy of Sciences, USA* 116: 8054–8059.

Hellens RP, Edwards EA, Leyland NR, Bean S, Mullineaux PM. 2000. pGreen: a versatile and flexible binary Ti vector for *Agrobacterium*-mediated plant transformation. *Plant Molecular Biology* 42: 819–832.

Hou Y, Zhai YI, Feng LI, Karimi HZ, Rutter BD, Zeng L, Choi DS, Zhang B, Gu W, Chen X *et al.* 2019. A *Phytophthora* effector suppresses trans-kingdom RNAi to promote disease susceptibility. *Cell Host & Microbe* 25: 153–165.

Huang C-H, Wang H, Hu P, Hamby R, Jin H. 2019. Small RNAs – big players in plant–microbe interactions. *Cell Host & Microbe* 26: 173–182.

Hudzik C, Hou Y, Ma W, Axtell MJ. 2020. Exchange of small regulatory RNAs between plants and their pathogens and parasites. *Plant Physiology* 182: 51–62.

Jahan SN, Asman AKM, Corcoran P, Fogelqvist J, Vetukuri RR, Dixelius C. 2015. Plant-mediated gene silencing restricts growth of the potato late blight pathogen *Phytophthora infestans*. *Journal of Experimental Botany* 66: 2785–2794.

Jia J, Lu W, Zhong C, Zhou R, Xu J, Liu W, Gou X, Wang Q, Yin J, Xu C *et al.* 2017. The 25–26 nt small RNAs in *Phytophthora parasitica* are associated with efficient silencing of homologous endogenous genes. *Frontiers in Microbiology* 8: 773.

Johnson NR, Yeoh JM, Coruh C, Axtell MJ. 2016. Improved placement of multi-mapping small RNAs. *G3 Genes| Genomes| Genetics* 6: 2103–2111.

Kreuze JF, Savenkov EI, Cuellar W, Li X, Valkonen JP. 2005. Viral class 1 RNase III involved in suppression of RNA silencing. *Journal of Virology* 79: 7227–7238.

Lakhotia N, Joshi G, Bhardwaj AR, Katiyar-Agarwal S, Agarwal M, Jagannath A, Goel S, Kumar A. 2014. Identification and characterization of miRNAome in root, stem leaf and tuber developmental stages of potato (*Solanum tuberosum* L.) by high-throughput sequencing. *BMC Plant Biology* 14: 6.

Langmead B, Salzberg S. 2012. Fast gapped-read alignment with BOWTIE2. *Nature Methods* 9: 357–359.

Leesutthiphonchai W, Vu AL, Ah-Fong AMV, Judelson HS. 2018. How does *Phytophthora infestans* evade control efforts? Modern insight into the late blight disease. *Phytopathology* 108: 916–924.

Li F, Pignatta D, Bendix C, Brunkard JO, Cohn MM, Tung J, Sin H, Kumar P, Baker B. 2012. MicroRNA regulation of plant innate immune receptors. *Proceedings of the National Academy of Sciences, USA* 109: 1790–1795.

Liao Z, Persson Hodén K, Singh KR, Dixelius C. 2020. Genome-wide identification of Argonautes in Solanaceae with emphasis on potato. *Scientific Reports* 10: 20577.

Lindbo JA. 2007. High-efficiency protein expression in plants from agoinfection-compatible *Tobacco mosaic virus* expression vectors. *BMC Biotechnology* 7: 52.

Liu L, Chen X. 2018. Intercellular and systemic trafficking of RNAs in plants. *Nature Plants* 4: 869–878.

Liu H, Yu X, Li K, Klejnot J, Yang H, Lisiero D, Lin C. 2008. Photoexcited CRY2 interacts with CIB1 to regulate transcription and floral initiation in *Arabidopsis*. *Science* 322: 1535–1539.

Livak KJ, Schmittgen TD. 2001. Analysis of relative gene expression data using real-time quantitative PCR and the $2^{-\Delta\Delta CT}$ method. *Methods* 25: 402–408.

Llorente B, Bravo-Almonacid F, Cvitanich C, Orlowska E, Torres HN, Flawia MM, Alonso GD. 2010. A quantitative real-time PCR method for *in planta* monitoring of *Phytophthora infestans* growth. *Letters in Applied Microbiology* 51: 603–610.

Matzke MA, Mosher RA. 2014. RNA-directed DNA methylation: an epigenetic pathway of increasing complexity. *Nature Review Genetics* 15: 394–408.

McCue A, Nuthikattu S, Slotkin RK. 2013. Genome-wide identification of genes regulated in trans by transposable element small interfering RNAs. *RNA Biology* 10: 1379–1395.

Mi S, Cai T, Hu Y, Chen Y, Hodges E, Ni F, Wu L, Li S, Zhou H, Long C *et al.* 2008. Sorting of small RNAs into *Arabidopsis* Argonaute complexes is directed by the 5′ terminal nucleotide. *Cell* 133: 116–127.

Mindrebo JT, Nartey MC, Seto Y, Burkart MD, Noel JP. 2016. Unveiling the functional diversity of the alpha/beta hydrolase superfamily in the plant kingdom. *Current Opinion in Structural Biology* 41: 233–246.

Nakagawa T, Suzuki T, Murata S, Nakamura S, Hino T, Maeo K, Tabata R, Kawai T, Tanaka K, Niwa Y *et al.* 2007. Improved gateway binary vectors: high-performance vectors for creation of fusion constructs in transgenic analysis of plants. *Bioscience, Biotechnology and Biochemistry* 71: 2095–2100.

Pearson W, Lipman D. 1988. Improved tools for biological sequence comparison. *Proceedings of the National Academy of Sciences, USA* 85: 2444–2448.

Persson Hodén K, Hu X, Martinez G, Dixelius C. 2021. smartPARE: an R package for efficient identification of true mRNA cleavage sites. *International Journal of Molecular Sciences* 28: 4267.

Petre B, Contreras MP, Bozkurt TO, Schattat MH, Sklenar J, Schornack S, Abd-El-Haliem A, Castells-Graells R, Lozano-Duran R, Dagdas YF *et al.* 2021. Host-interactor screens of *Phytophthora infestans* RXLR proteins reveal vesicle trafficking as a major effector-targeted process. *Plant Cell* 33: 1147–1471.

Pumplin N, Voinnet O. 2013. RNA silencing suppression by plant pathogens: defence, counter-defence and counter-counter-defence. *Nature Reviews Microbiology* 11: 745–760.

Qiao Y, Liu L, Xiong Q, Flores C, Wong J, Shi J, Wang X, Liu X, Xiang Q, Jiang S *et al.* 2013. Oomycete pathogens encode RNA silencing suppressors. *Nature Genetics* 45: 330–333.

Qiao Y, Shi J, Zhai Y, Hou Y, Ma W. 2015. Phytophthora effector targets a novel component of small RNA pathway in plants to promote infection. *Proceedings of the National Academy of Sciences, USA* 112: 5850–5855.

Qutob D, Chapman BP, Gijzen M. 2013. Transgenerational gene silencing causes gain of virulence in a plant pathogen. *Nature Communications* 4: 1349.

Ren B, Wang X, Duan J, Ma J. 2019. Rhizobial tRNA-derived small RNAs are signal molecules regulating plant nodulation. *Science* 365: 919–922.

Rogers K, Chen X. 2013. Biogenesis, turnover, and mode of action of plant microRNAs. *Plant Cell* 25: 2383–2399.

Shivaprasad PV, Chen HM, Patel K, Bond DM, Santos BACM, Baulcombe DC. 2012. A microRNA superfamily regulates nucleotide binding site-leucine-rich repeats and other mRNAs. *Plant Cell* 24: 859–874.

Stamatakis A. 2006. RAxML-VI-HPC: maximum likelihood-based phylogenetic analyses with thousands of taxa and mixed models. *Bioinformatics* 22: 2688–2690.

The Potato Genome Sequencing Initiative. 2011. Genome sequence and analysis of the tuber crop potato. *Nature* 475: 189–195.

Théry C. 2011. Exosomes: secreted vesicles and intercellular communications. *F1000 Biology Reports* 3: 15.

Thieme CJ, Schudoma C, May P, Walther D. 2012. Give if AGO: the search for miRNA-Argonaute sorting signals in *Arabidopsis thaliana* indicates a relevance of sequence positions other than the 5′-position alone. *Frontiers of Plant Science* 3: 272.

Todesco M, Rubio-Somoza I, Paz-Ares J, Weigel D. 2010. A collection of target mimics for comprehensive analysis of microRNA function in *Arabidopsis thaliana*. *PLoS Genetics* 6: e1001031.

Varkonyi-Gasic E, Wu R, Wood M, Walton EF, Hellens RP. 2007. Protocol: a highly sensitive RT-PCR method for detection and quantification of microRNAs. *Plant Methods* 3: 12.

Vetukuri RR, Åsman AKM, Tellgren-Roth C, Jahan SN, Reimegård J, Fogelqvist J, Savenkov E, Söderbom F, Avrova AO, Whisson SC *et al.* 2012. Evidence for small RNAs homologous to effector-encoding genes and transposable elements in the oomycete *Phytophthora infestans*. *PLoS ONE* 7: e51399.

Vetukuri RR, Avrova AO, Grenville-Briggs LJ, Van West P, Söderbom F, Savenkov EI, Whisson SC, Dixelius C. 2011. Evidence for involvement of Dicer-like, Argonaute and histone deacetylase proteins in gene silencing in *Phytophthora infestans*. *Molecular Plant Pathology* 12: 772–785.

de Vries S, Kukuk A, von Dahlen KJ, Schanke A, Kloesges T, Rose EL. 2018. Expression profiling across wild and cultivated tomatoes supports the relevance of early miR484/2118 for *Phytophthora* resistance. *Proceedings Royal Society B* 285: 20172560.

Wang Q, Li T, Zhong C, Luo S, Xu K, Gu B, Meng Y, Tyler BM, Shan W. 2019. Small RNAs generated by directional transcription mediate silencing of RXLR effector genes in the oomycete *Phytophthora sojae*. *Phytopathology Research* 1: 18.

Wang S, McLellan H, Bukharova T, He Q, Murphy F, Shi J, Sun S, van Weymers P, Hein I, Wang X *et al.* 2019. *Phytophthora infestans* RXLR effectors act in concert at diverse subcellular locations to enhance host colonization. *Journal of Experimental Botany* 70: 343–356.

Weiberg A, Wang M, Lin F-M, Zhao H, Zhang Z, Kaloshian I, Huang H-D, Jin H. 2013. Fungal small RNAs suppress plant immunity by hijacking host RNA interference pathways. *Science* 342: 118–123.

Whisson SC, Avrova AO, Vetukuri RR, Dixelius C. 2012. Can silencing of transposons contribute to diversity of pathogenicity and virulence in *Phytophthora*? *Mobile Genetic Elements* 2: 110–114.

Whisson SC, Boevink PC, Wang S, Birch PRJ. 2016. The cell biology of late blight disease. *Current Opinion of Microbiology* 34: 127–135.

Xiong Q, Ye W, Choi D, Wong J, Qiao Y, Tao K, Wang Y, Ma W. 2014. *Phytophthora* suppressor of RNA silencing 2 is a conserved RxLR effector that promotes infection in soybean and *Arabidopsis thaliana*. *Molecular Plant–Microbe Interactions* 27: 1379–1389.

Yan Y, Ham B-K, Chong YH, Lucas Y-D. 2020. A plant small RNA-binding protein 1 family mediates cell-to cell trafficking of RNAi signals. *Molecular Plant* 13: 321–335.

Yang X, Dong W, Ren W, Zhao Q, Wu F, He Y. 2021. Cytoplasmic HYL1 modulates miRNA-mediated translational repression. *Plant Cell* 33: 1980–1996.

Yang Z. 2007. PAML 4: phylogenetic analysis by maximum likelihood. *Molecular Biology and Evolution* 24: 1586–1591.

Yoo BC, Kragler F, Varkonyi-Gasic E, Haywood V, Archer- Evans S, Lee YM, Lough TJ, Lucas WJ. 2004. A systemic small RNA signaling system in plants. *Plant Cell* 16: 1979–2000.

Yoshida K, Schuenemann VJ, Cano LM, Pais M, Mishra B, Sharma R, Lanz C, Martin FN, Kamoun S, Krause J *et al.* 2013. The rise and fall of the *Phytophthora infestans* lineage that triggered the Irish potato famine. *eLife* 2: e00731.

Zhang T, Zhao Y-L, Zhao J-H, Wang S, Jin Y, Chen Z-Q, Fang Y-Y, Hua C-L, Ding S-W, Guo H-S. 2016. Cotton plants export microRNAs to inhibit virulence gene expression in a fungal pathogen. *Nature Plants* 2: 16153.

Supporting Information

Additional Supporting Information may be found online in the Supporting Information section at the end of the article.

Fig. S1 Relative *Phytophthora infestans* DNA content in infected potato.

Fig. S2 Pipeline for the bioinformatics analysis.

Fig. S3 Individual replicates of small RNAs derived from co-immunoprecipitated-enriched RNA samples.

Fig. S4 5′ nt distribution of *Pi*-sRNAs derived from co-immunoprecipitated-enriched RNA samples.

Fig. S5 Predicted sRNA target mRNAs.

Fig. S6 sRNA subgroups targeting resistance genes in the potato genome.

Fig. S7 *PITG_10391* and miR8788 potato target candidate assay.

Fig. S8 Genomic sequence comparisons of miR8788.

Fig. S9 Secondary structure of pre-miR8788.

Fig. S10 Chromosomal distribution of predicted potato phasiRNAs.

Fig. S11 SHORTSTACK prediction of miR8788 in the *pHAM34: PiAgo1-GFP* mycelia samples.

Fig. S12 StABH1 analysis.

Fig. S13 Subcellular localization of *St*ABH1.

Fig. S14 Phylogeny of alpha/beta hydrolase-type proteins (collapsed).

Fig. S15 Phylogeny of alpha/beta hydrolase-type proteins.

Fig. S16 Multiple sequence alignment of the *StABH1* coding sequence in different potato cultivars.

Table S1 Oligo sequences for rapid amplification of cDNA ends, constructs and Northern blots.

Table S2 Quantitative reverse transcription polymerase chain reaction primer sequences.

Table S3 sRNAs predicted to target the same resistance genes in the potato genome.

Table S4 Predicted miR8788 target transcripts in the *P. infestans* genome.

Please note: Wiley Blackwell are not responsible for the content or functionality of any Supporting Information supplied by the authors. Any queries (other than missing material) should be directed to the *New Phytologist* Central Office.

About *New Phytologist*

- *New Phytologist* is an electronic (online-only) journal owned by the New Phytologist Foundation, a **not-for-profit organization** dedicated to the promotion of plant science, facilitating projects from symposia to free access for our Tansley reviews and Tansley insights.

- Regular papers, Letters, Viewpoints, Research reviews, Rapid reports and both Modelling/Theory and Methods papers are encouraged. We are committed to rapid processing, from online submission through to publication 'as ready' via *Early View* – our average time to decision is <26 days. There are **no page or colour charges** and a PDF version will be provided for each article.

- The journal is available online at Wiley Online Library. Visit **www.newphytologist.com** to search the articles and register for table of contents email alerts.

- If you have any questions, do get in touch with Central Office (np-centraloffice@lancaster.ac.uk) or, if it is more convenient, our USA Office (np-usaoffice@lancaster.ac.uk)

- For submission instructions, subscription and all the latest information visit **www.newphytologist.com**